Optical spectra and intensities of graphene magnetic dot bound to a negatively charged Coulomb impurity

Lee, C. M.; Chan, K. S.

Published in:
Journal of Applied Physics

Published: 28/07/2014

Document Version:
Final Published version, also known as Publisher's PDF, Publisher's Final version or Version of Record

Published version (DOI):
10.1063/1.4891886

Publication details:
Lee, C. M., & Chan, K. S. (2014). Optical spectra and intensities of graphene magnetic dot bound to a negatively charged Coulomb impurity. *Journal of Applied Physics*, *116*(4), Article 43712. https://doi.org/10.1063/1.4891886

Optical spectra and intensities of graphene magnetic dot bound to a negatively charged Coulomb impurity

Cite as: J. Appl. Phys. **116**, 043712 (2014); https://doi.org/10.1063/1.4891886
Submitted: 23 May 2014 • Accepted: 21 July 2014 • Published Online: 31 July 2014

C. M. Lee and K. S. Chan

Optical spectra and intensities of graphene magnetic dot bound to a negatively charged Coulomb impurity

C. M. Lee[1,2,a)] and K. S. Chan[1,2,a)]
[1]*Department of Physics and Materials Science and Center for Functional Photonics, City University of Hong Kong, Tat Chee Avenue, Kowloon, Hong Kong, People's Republic of China*
[2]*Shenzhen Research Institute, City University of Hong Kong, Shenzhen, People's Republic of China*

(Received 23 May 2014; accepted 21 July 2014; published online 31 July 2014)

Employing numerical diagonalization, we study the optical properties of an electron in a monolayer-graphene magnetic dot bound to an off-center negatively charged Coulomb impurity based on the massless Dirac-Weyl model. Numerical results show that, since the electron-hole symmetry is broken by the Coulomb potential, the optical absorption spectra of the magnetic dot in the presence of a Coulomb impurity are different between the electron states and the hole states. Effects of both the magnetic field and the dot size on the absorption coefficient are presented as functions of the incident photon energies. © *2014 AIP Publishing LLC*.
[http://dx.doi.org/10.1063/1.4891886]

I. INTRODUCTION

Earlier in the past two decades, quantum dots, involving few electrons confined electrically or/and magnetically in semiconductor structures, were a subject being intensely studied in condensed matter physics[1] since the great progresses in nanofabrication techniques. Recently, the isolation of stable monolayer and few-layer graphene sheets by Novoselov *et al.*[2,3] has aroused considerable interest in the study of their electronic properties.[3–7] These graphene systems exhibit extraordinary properties, including the linear energy-momentum dispersion at low energies of the massless relativistic fermions, which are well governed by the Dirac-Weyl (DW) model, rather than the nonrelativistic Schrödinger model as appropriate for those semiconductor materials.

Owing to the Klein tunneling,[8] the charged Dirac electrons in graphene cannot be confined by electrostatic barriers. The so-called magnetic dot, rather than the quantum dot, in which electrons are confined purely by nonuniform magnetic fields, becomes one of the research foci in graphene in the exploration of fascinating quantum properties for potential high-density memory and spintronic device applications. Systems of different field configurations without and with impurities were considered to confine electrons which include sequences of alternating magnetic barriers and wells,[9] exponentially decaying fields,[10] non-zero or zero fields in a circular dot,[11–13] fields corresponding to various potentials,[14] circular step fields,[15] Guassian fields,[16] ring fields,[17] and even in the presence of rather general potential terms which arise intentionally or from impurities.[18–22] All these studies focus on the field dependences of the low-lying spectra and the energy dependences of the transmission probability through the magnetic field barriers, and the electron states including bound, quasi-bound, and scattering states. As a whole, they all concluded that electrons can be confined by the magnetic barriers in graphene.

In experiment, spectroscopic techniques provide convenient tools for exploring the electronic states of quantum dots. In particular, their electronic structures can be studied through those allowed intraband transitions when different polarizations of radiation are considered. In some previous theoretical studies, the foci are on the Schrödinger model of the impurities in low dimensional structures.[23,24] Properties related to the optical intensities, including the photoionization cross section,[25–27] the nonlinear optical coefficient,[28,29] and even related to the Raman scattering,[30–32] were discussed in detail. They concluded that the optical intensities for intraband transitions strongly depend on the magnetic field and the quantum dot size. However, the studies of the above-mentioned problems in the DW model are rare.

In our present study, a two-dimensional (2D) magnetic dot created by a nonuniform field of the Gaussian type is considered. Starting from the DW Hamiltonian of the single electron magnetic dot system in the presence of an off-center negatively charged Coulomb impurity, we calculate the absorption coefficient for intraband transitions as a function of the incident photon energy using those states with eigenvalues and eigenvectors obtained by numerical diagonalization. In order to show the impurity effect on the absorption coefficient, we focus on four typical low-lying states $|n, l\rangle$ with the same radial quantum number n, i.e., $|1, 0\rangle$, $|1, \pm 1\rangle$, and $|1, -2\rangle$ of both the electron and hole states, as examples for demonstration. The transition absorption intensities between those states with different n are several order of magnitude lower and are therefore neglected. Finally, we compare the intraband absorption coefficient with and without an impurity, and analyse the impurity effect with the confining properties of the magnetic dot for such a DW model.

II. THEORY

In the framework of the massless DW model, the Hamiltonian describing a single electron bound to an

a)Authors to whom correspondence should be addressed. Electronic addresses: C. M. Lee: mesimon_hk@yahoo.com.hk and K. S. Chan: apkschan@cityu.edu.hk. Tel.: 852 3442-7831. Fax: 852 3442-0538.

off-center negatively charged Coulomb impurity in a 2D monolayer graphene based magnetic dot formed by a non-uniform magnetic field reads

$$\hat{H} = v_F \sigma \cdot (\mathbf{P} + e\mathbf{A}) + \mathbf{I}\frac{e^2}{4\pi\epsilon\sqrt{r^2+d^2}}, \tag{1}$$

where v_F is the electron's Fermi velocity instead of the photon's in the conventional Dirac equation. $\sigma = (\sigma_x, \sigma_y)$ are the 2×2 Pauli matrices in the pseudo-spin space, and $\mathbf{I}$ is the identity matrix. $\mathbf{P}$ and $\mathbf{A}$ are the momentum operator and the vector potential in the 2D space, respectively. The last term is the Coulomb interaction, depending on the separation d between the impurity and the plane of the magnetic dot, and the positive sign means the interaction between the electron and the impurity is repulsive. In the present case, we choose the Gaussian function as the profile of the magnetic field, $B_0(1-\exp(-r^2/r_0^2))$, which is perpendicular to the xy dot plane. In such a profile, the field value is zero at the dot center and increases exponentially from zero up to the maximum B_0 at sufficiently large r. The corresponding vector potential $\mathbf{A}$ is then represented in the polar coordinate by

$$\mathbf{A} = \left\{\frac{B_0 r}{2} - \frac{B_0 r_0^2}{2r}\left[1 - \exp\left(-\frac{r^2}{r_0^2}\right)\right]\right\}\hat{\mathbf{e}}_\theta, \tag{2}$$

where $\hat{\mathbf{e}}_\theta$ is the unit vector in the azimuthal direction. In order to calculate the eigenenergy of the whole system by numerical diagonalization, the Hamiltonian [Eq. (1)] is decomposed into two parts

$$\hat{H} = \hat{H}_0 + \hat{V}, \tag{3}$$

so that the unperturbed one is a 2×2 matrix block denoting that the electron moves under a uniform field B in the absence of Coulomb impurity, which can be expressed as follows:

$$\hat{H}_0 = v_F\begin{pmatrix} 0 & \hat{\pi}_0^- \\ \hat{\pi}_0^+ & 0 \end{pmatrix}, \tag{4}$$

with the operators

$$\hat{\pi}_0^{\pm} = \pm j\exp(\pm j\theta)\left[\mp\hbar\frac{\partial}{\partial r} + \frac{l\hbar}{r} + \frac{erB}{2}\right], \tag{5}$$

where $\hat{H}_0$ is analytically solvable, yielding the well-known 2D harmonic product basis states as eigenfunction for both components of the spinor. The two-component spinor $\Psi_{nl}^T = (\phi_{N-1,l-1} \;\; j\phi_{N,l})$ has the two components corresponding to the sublattices of graphene. $N[\equiv n + (l+|l|)/2]$ is the nonnegative integer Landau level (LL) index, and $E_{N,l} = \pm N^{\frac{1}{2}}$ are the two eigenvalues in energy unit of $\hbar\omega(\equiv\sqrt{2}v_F\hbar/a)$. n and $l\hbar$ are the radial quantum number and the orbital angular momentum, respectively. $L_n^{|l|}$ and $a(\equiv\sqrt{\hbar/eB})$ are the associated Laguerre polynomials and the magnetic length, respectively. As can be seen from the eigenvalues in the case of uniform fields, $\hat{\pi}_0^-$ and $\hat{\pi}_0^+$ can be regarded as lowering and raising operators, respectively, since they operate on the two-component spinor to give the following: $\hat{\pi}_0^+\phi_{N-1,l-1} = \sqrt{N}\phi_{N,l}$ and $\hat{\pi}_0^-\phi_{N,l} = \sqrt{N}\phi_{N-1,l-1}$. Note that each LL is highly degenerate and consists of infinite quantum states with various orbital angular momenta l. In order to differentiate them from the bulk LL, these discrete quantum states split from the bulk LL under non-uniform magnetic fields are called the angular momentum states.

In Eq. (3), the residual potential can be expressed as the 2×2 matrix block of the last term, $\hat{V}$, and explicitly given by

$$\hat{V} = \begin{pmatrix} \hat{V}_{\text{coul}} & \hat{V}_+ \\ \hat{V}_- & \hat{V}_{\text{coul}} \end{pmatrix}, \tag{6}$$

in which the diagonal and non-diagonal elements, respectively, are given in dimensionless units by

$$\hat{V}_{\text{coul}} = \frac{C}{\sqrt{r^2+d^2}}, \tag{7}$$

$$\hat{V}_{\pm} = \mp j\exp(\mp j\theta)\times\frac{-F(r)}{2\sqrt{2}r}, \tag{8}$$

with

$$F(r) = r_0^2\left[1 - \exp\left(-\frac{r^2}{r_0^2}\right)\right], \tag{9}$$

where the Coulomb parameter C, in units of magnetic length a, represents the interaction strength of the electron with the on-center impurity, and is given by

$$C = \frac{e^2}{2\sqrt{2}\epsilon v_F h}. \tag{10}$$

In the numerical calculation, the size of the model space for such a 2×2 matrix block [Eq. (6)] includes 30 pairs of low basis states for a particular orbital angular momentum l, since the ratio of the difference in eigenenergy is less than 0.001% for the further increase of the number of basis states. Next, in order to calculate the intraband absorption spectrum within the electric-dipole approximation, we define the absorption coefficient for the transition between two states as[23,24]

$$\alpha(\hbar\omega) \propto \sum_f |\langle n_f, l_f|r\exp(\pm j\theta)|n_i, l_i\rangle|^2\hbar\omega\delta(\hbar\omega - |E_f - E_i|), \tag{11}$$

with a Lorentzian function,[27] with lifetime width Γ_f, expressed by

$$\delta(\hbar\omega - |E_f - E_i|) = \frac{\Gamma_f}{\pi\left[(\hbar\omega - |E_f - E_i|)^2 + \Gamma_f^2\right]}, \tag{12}$$

where $\hbar\omega$ is the incident photon energy. $|n_i, l_i\rangle$ and $|n_f, l_f\rangle$ are the wavefunctions of the initial and the final states, and E_i and E_f are the corresponding energy eigenvalues of these states, respectively. These states with their eigenvalues are obtained previously by numerical diagonalization. In Eq. (11), the matrix element $|\langle n_f, l_f|r\exp(\pm j\theta)|n_i, l_i\rangle|$ is the

overlapping of the wavefunctions of the initial state and final state, and the ± sign refers to the circular left/right polarization of the light. The presence of the phase factor $\exp(\pm j\theta)$ leads to the following selection rule: the matrix element is non-zero only for transitions in which the angular momentum changes by one unit, i.e., $\Delta l = \pm 1$. In the present study, transitions between states with different quantum numbers n are neglected since these transitions are at least several orders of magnitude weaker in intensities. In order to show the effect of Coulomb impurity on the absorption spectra, we focus on four states $|1, 0\rangle$, $|1, \pm 1\rangle$, and $|1, -2\rangle$ for intraband transitions. Positive- and negative-energy states are included and calculated separately for comparison.

III. DISCUSSION AND CONCLUSIONS

In our present calculation, the Coulomb parameter is set to be $C = 0.5$ and 0.8 with the separation between the impurity and the dot plane $d = 0.5r_0$ or $0.5a$.[16] The different separations d are not considered in this study since their effect on the energy spectra is similar to that of the Coulomb parameter. The value of the lifetime width is fixed to be $0.02E_0$ for simplicity, where $E_0 = \sqrt{2}\hbar v_F/r_0$ or $\sqrt{2}\hbar v_F/a$ for the dot size or magnetic field being fixed. Its actual value depends on several factors including temperature and pressure. In the figures, the states are labeled by $(n, l)^{\pm}$ for clear identification, in which the superscripts "+" and "−" represent the positive (or electron) and the negative (or hole) energy states, respectively.

We study the effect of the Coulomb impurity on the intraband absorption coefficient primarily based on their quantum states for transitions. Figures 1 and 2 show all four states, without and with negatively charged Coulomb impurity, studied in this work as functions of the magnetic field and dot size, respectively. Note that the states for the lowest LL ($N = 0$) are not considered; it is because this original highly degenerate energy level splits into discrete angular momentum states only when the Coulomb potential due to charged impurity is present. It is expected that the peaks of absorption coefficient for these intraband transitions just shift to higher energies without any other special features, and therefore are no longer discussed in the present study.

Starting from the impurity-free case. In Figs. 1(a) and 2(a), both energy spectra have symmetrical structures about the horizontal axis. Owing to the electron-hole symmetry, we only discuss the positive energy states. At sufficiently weak magnetic fields, the angular momentum states are in general far from the magnetic edge or the dot center. The electron moves with an analogy to that in a uniform field, and therefore the states resemble the bulk LL. When the field increases [Fig. 1(a)], its confinement pushes the states closer to the dot region, where the magnetic field is lower, leading their eigenenergies to deviate downward from their corresponding bulk LLs. Also the stronger the field, the larger the spacing between the angular momentum states is. For a given LL under a certain field, the lower the angular momentum $|l|$, the closer the state is toward the dot region, and hence the larger its eigenenergy deviates from the bulk LL. These overall energy shifts lead to the splitting of the discrete angular momentum states. As can be observed from Fig. 3(a), the absorption coefficients overall have blue shifts to higher photon energies and also have stronger peaks when the field increases. Fig. 2(a) shows the dot-size dependent spectra under a fixed field. When the dot size increases, the electron moves at the low-field dot region more probably. And its eigenenergies for the angular momentum states, similar to that of field-dependent spectra, become lower and deviate further away from its corresponding bulk LL at different rates. From the inset of Fig. 3(b), it can be seen clearly that, when the dot size increases, the differences in

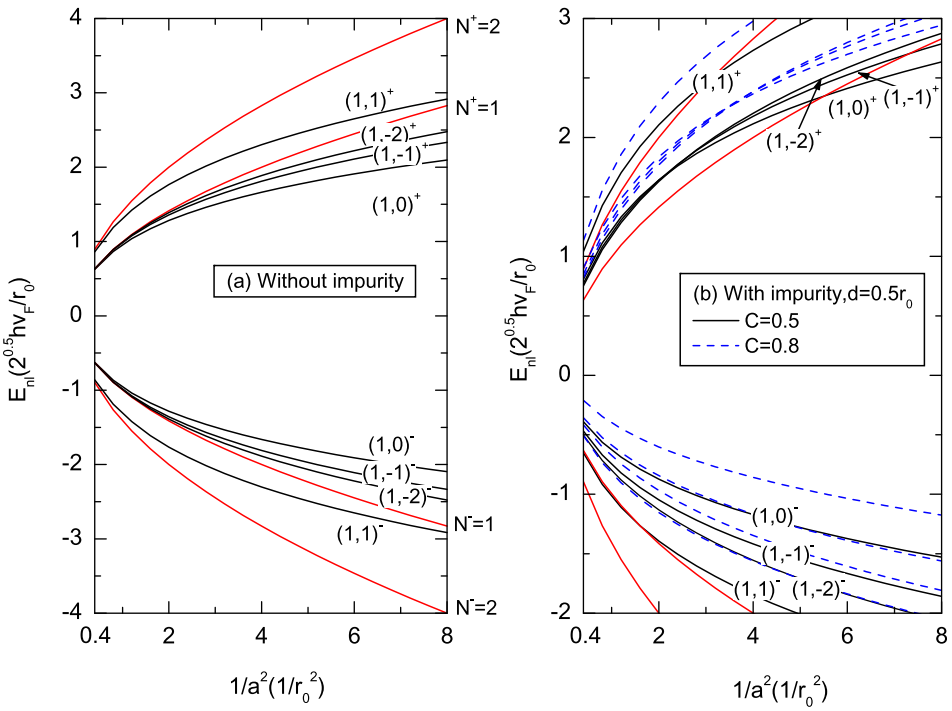

FIG. 1. Energy levels of the states (1, 0), (1, ±1), and (1, −2), including electron and hole states, as functions of the magnetic field $B \propto 1/a^2$, (a) without impurity and (b) with impurity using two values of Coulomb parameter, $C = 0.5$ and 0.8, noting that the bulk LLs denoted by solid curves in red are drawn for comparison.

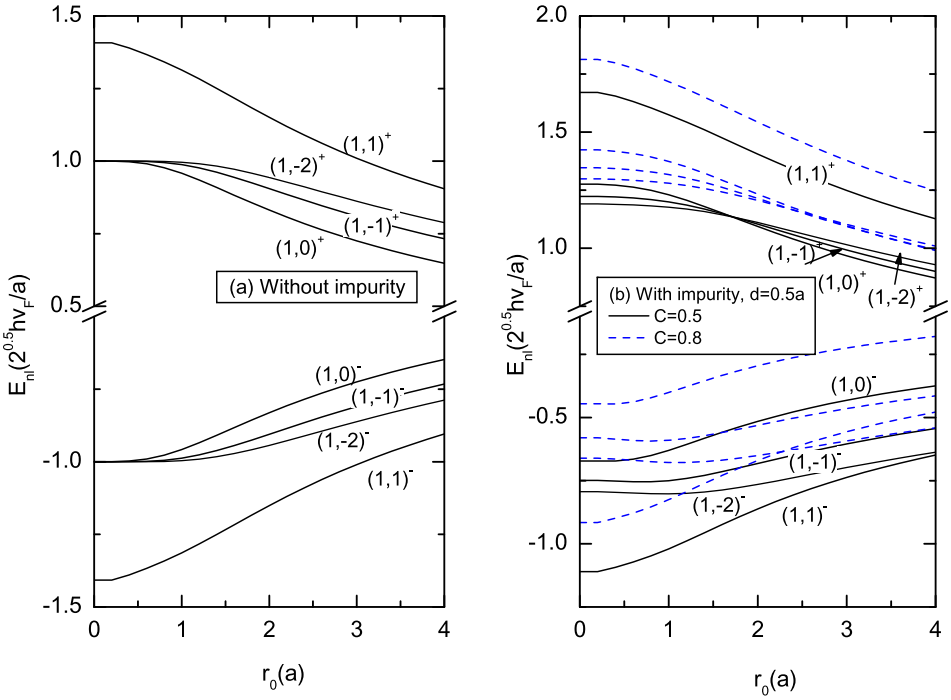

FIG. 2. Energy levels of the states (1, 0), (1, ±1), and (1, −2), including electron and hole states, as functions of the dot size, (a) without impurity and (b) with impurity using two values of Coulomb parameter, $C = 0.5$ and 0.8.

eigenenergies between $l = 0$ and -1 and between $l = -1$ and -2 increase but that between $l = 0$ and 1 decreases. Therefore, the absorption coefficients for the former cases have blue shift while that for $l = 0 \rightarrow 1$ has red shift, and finally tails of these two peaks overlap partly at sufficiently large dot size, $r_0 = 4a$.

Let us now consider the case of negatively charged impurity. We see from Figs. 1(b) and 2(b) that the spectra for both the magnetic-field and the dot-size dependences are shifted upward, and the electron-hole symmetry is broken. In the positive-energy states, for $N^+ = 1$, there exist a critical magnetic field [$r_0^2/a^2 \approx 2$ for $C = 0.5$, and ≈ 3 for $C = 0.8$, see Fig. 1(b)] and a critical dot size [$r_0 \approx 1.75a$ for $C = 0.5$, and $\approx 2.5a$ for $C = 0.8$, see Fig. 2(b)] for level crossings between $(1, -2)^+$, $(1, -1)^+$, and $(1, 0)^+$. In the electron-impurity interacting system, there are two interacting energies with opposite effects on the ordering of these states for the first LL ($N^+ = 1$), one is repulsive Coulomb force of the negatively charged impurity and the other is the inhomogeneous field confinement, which compete with each other. As to be known that, when the Coulomb effect is considered, the state $(1, 0)^+$ has much higher eigenenergy comparing

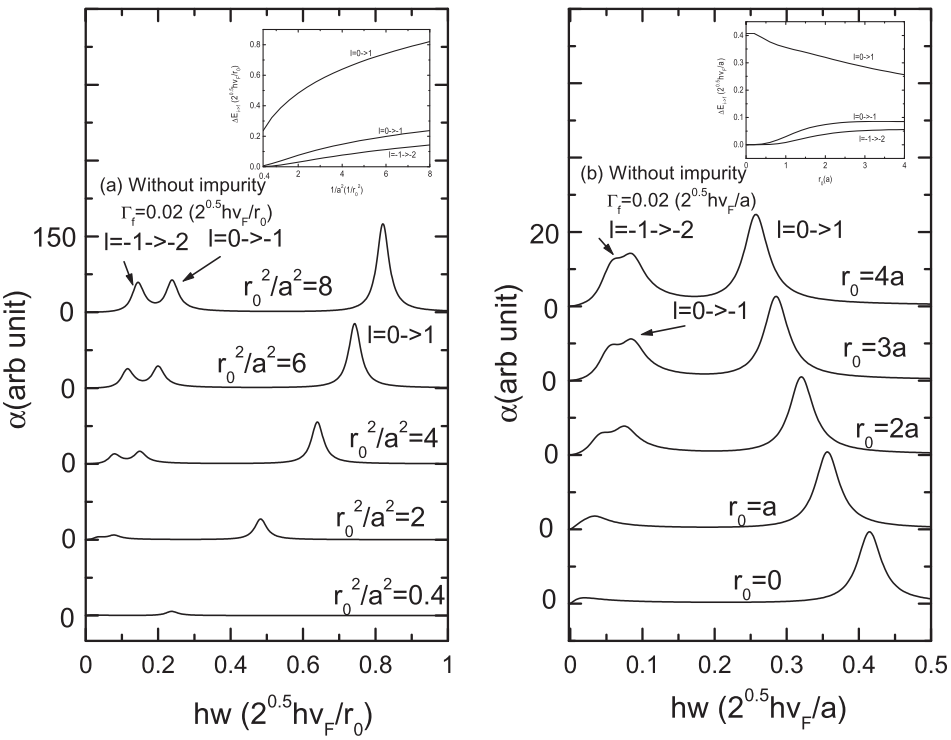

FIG. 3. Absorption spectra due to intraband $|1, 0\rangle \rightarrow |1, 1\rangle$, $|1, 0\rangle \rightarrow |1, -1\rangle$, and $|1, -1\rangle \rightarrow |1, -2\rangle$ transitions for impurity-free case, with (a) different magnetic fields and (b) different dot sizes, noting that the insets show energy differences between two states for transitions.

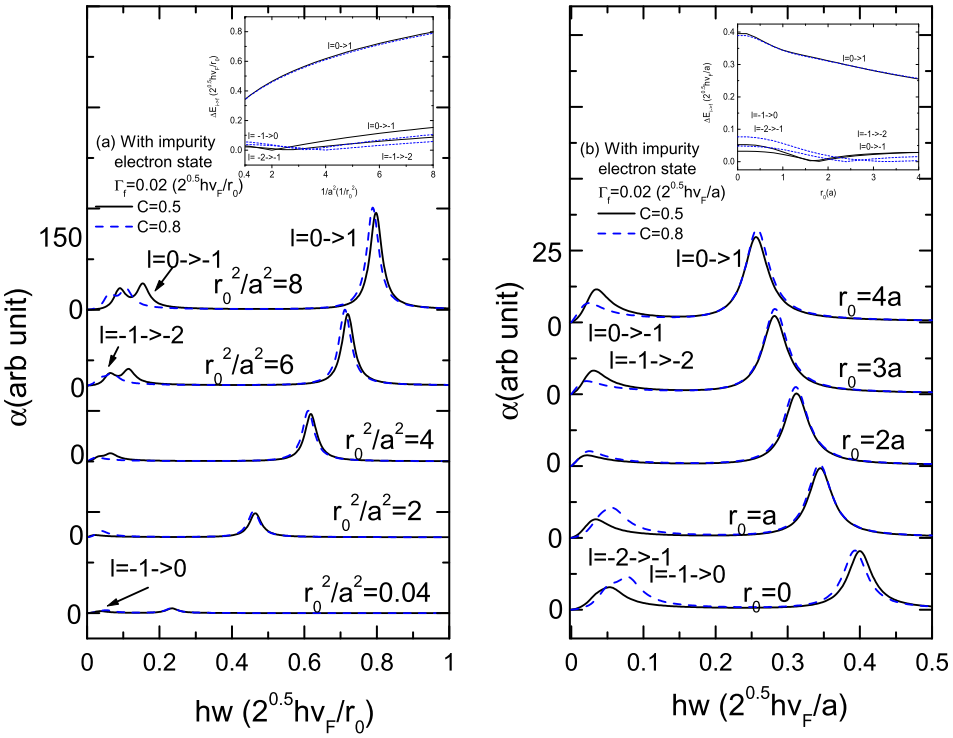

FIG. 4. Same as those in Fig. 3 but for the electron states with impurity using two values of Coulomb parameter $C = 0.5$ and 0.8.

with $(1, -1)^+$ or $(1, -2)^+$, since the former is much closer to the impurity and experiences larger repulsive force from it. This argument comes true for the field below the critical value [Fig. 1(b)], when the field confinement is not strong. It is also true when the dot size is not large [Fig. 2(b)], since the effect due to the inhomogeneous field is not significant. Above the critical values, the level ordering returns to those of the impurity-free case and the field confinement returns to be much dominant. Figs. 4(a) and 4(b) show the absorption coefficient for the transitions between these states as functions of incident photon energy for different fields and different dot sizes, respectively. As can be clearly seen from the figures that the peaks have red shifts toward zero photon energy and turn to vanish at around the critical field or critical dot size. This is one of the obvious experimental evidences for the presence of impurities in such an electron interacting system. It is worth noting that the intraband transitions below and above these critical values are just reversed, i.e., from $l = -1 \rightarrow 0$ to $l = 0 \rightarrow -1$, and from $l = -2 \rightarrow -1$ to $l = -1 \rightarrow -2$. This phenomena cannot be

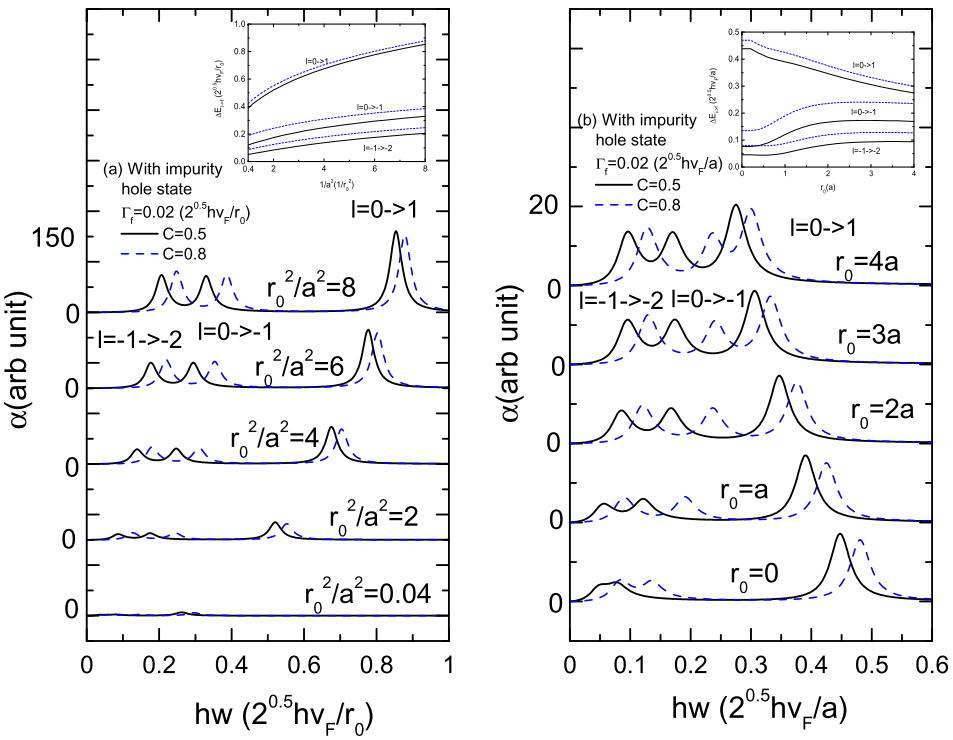

FIG. 5. Same as those in Fig. 3 but for the hole states with impurity using two values of Coulomb parameter $C = 0.5$ and 0.8.

observed in $l=0 \rightarrow 1$ transition. Instead, the peak has blue shift to higher photon energy with increasing magnetic field [Fig. 4(a)] but has red shift to lower photon energy with decreasing dot size [Fig. 4(b)], without vanishing in between.

In the negative-energy states [Figs. 1(b) and 2(b)], the reverse level ordering or crossing features with critical points found in the positive energy states cannot be observed since the Coulomb potential and the field confinement have similar effect to push the states toward the dot center. The states in turn separate further apart in eigenenergies instead as compared with the positive energy states. From the absorption spectra in Fig. 5, we see that the peaks for both $l=0 \rightarrow -1$ and $l=-1 \rightarrow -2$ transitions are shifted to higher photon energy when the Coulomb parameter increases. Apart from this, overall, the absorption coefficients for both the field and the dot-size dependences are similar to those of the impurity-free cases [Fig. 3].

Two more notes to be made, in the present entire study, are that (1) regardless of the presence of impurity, the peaks for the intraband transitions between the states of the same LL in the negative-energy states can be well resolved and are largely affected by the Coulomb strength, while those in the positive-energy states cannot, and (2) in order to demonstrate the formation of confined states in a graphene magnetic dot, the main focus in experiments is on those states lying in very low density of state (DOS) regions, since it can give well resolved peaks in the absorption spectra. The stronger the Coulomb interaction strength, the further the states are away from their corresponding highly degenerate LLs, particularly for hole states, see Fig. 5 and zero LL in Ref. 16, and more well resolved peaks we can get finally. In other word, well resolved peaks can be obtained by using large Coulomb parameter C and small separation d.

In summary, using direct diagonalization, we theoretically investigate optical intensities for intraband transitions between $|1,0\rangle$, $|1,\pm1\rangle$, and $|1,-2\rangle$ for a 2D graphene magnetic dot under the influence of an off-center negatively charged Coulomb impurity. The effects of both the magnetic field and the dot size are taken into account in the calculation. Several concluding remarks are given as follows:

(a) In the absence of impurity, the evolutions of the absorption coefficient for the electron states and the hole states are similar regardless of the magnetic field or the dot size, since the whole spectra show a hole-electron symmetrical structure about the horizontal axis.
(b) With an off-center negatively charged impurity, the evolutions of the absorption coefficient for the electron states and the hole states are different, and its value in the electron state turns to zero at critical fields or critical dot sizes. At the critical values, the level ordering within a given LL ($N=1$) is reversed owing to the competition between the repulsive Coulomb potential and the magnetic confinement.
(c) If the impurity is replaced by the positively charged one, it is expected that the evolutions of the absorption coefficient for the electron states and the hole states are just reversed. The point of level reverse ordering and the corresponding vanishing absorption coefficient now appears in the hole states. Overall, we conclude that optical spectroscopy is a suitable tool for verifying the existence of charged impurities in such magnetic dot systems. The present numerical results for the massless Dirac model will stimulate further studies on the same problem with more than one charged Coulomb impurities.

ACKNOWLEDGMENTS

This work was supported by City University of Hong Kong, under Project No. 7004007 and National Natural Science Foundation of China (NSFC, Grant No. 11274260).

[1]L. Jacak, P. Hawrylak, and A. Wojs, *Quantum Dots* (Springer-Verlag, Berlin, 1998); D. Bimberg, M. Grundmann, and N. N. Ledentsov, *Quantum Dot Heterostructures* (Wiley, Chichester, 1999); T. Chakraborty, *Quantum Dot* (Elsevier, Amsterdam, 1999).
[2]K. S. Novoselov, A. K. Geim, S. V. Morozov, D. Jiang, Y. Zhang, S. V. Dubonos, I. V. Grigorieva, and A. A. Firsov, Science **306**, 666 (2004).
[3]K. S. Novoselov, A. K. Geim, S. V. Morozov, D. Jiang, M. I. Katsnelson, I. V. Grigorieva, S. V. Dubonos, and A. A. Firsov, Nature **438**, 197 (2005).
[4]D. Gunlycke, H. M. Lawler, and C. T. White, Phys. Rev. B **75**, 085418 (2007).
[5]A. V. Rozhkov, G. Giavaras, Y. P. Bliokh, V. Freilikher, and F. Nori, Phys. Rep. **503**, 77 (2011).
[6]Y. Zhang, Y. W. Tan, H. L. Stormer, and P. Kim, Nature **438**, 201 (2005).
[7]K. S. Novoselov, Z. Jiang, Y. Zhang, S. V. Morozov, H. L. Stormer, U. Zeitler, J. C. Maan, G. S. Boebinger, P. Kim, and A. K. Geim, Science **315**, 1379 (2007).
[8]O. Klein, Z. Phys. **53**, 157 (1929).
[9]L. Dell'Anna and A. De Martino, Phys. Rev. B **79**, 045420 (2009).
[10]T. K. Ghosh, J. Phys.: Condens. Matter **21**, 045505 (2009).
[11]A. De Martino, L. Dell'Anna, and R. Egger, Phys. Rev. Lett. **98**, 066802 (2007).
[12]D. L. Wang and G. J. Jin, Phys. Lett. A **373**, 4082 (2009).
[13]C. M. Lee and K. S. Chan, J. Appl. Phys. **114**, 143708 (2013).
[14]S. Kuru, J. M. Negro, and L. M. Nieto, J. Phys.: Condens. Matter **21**, 455305 (2009).
[15]M. R. Masir, A. Matulis, and F. M. Peeters, Phys. Rev. B **79**, 155451 (2009).
[16]C. M. Lee and K. S. Chan, Solid State Commun. **185**, 52 (2014).
[17]C. M. Lee and K. S. Chan, J. Phys. Soc. Jpn. **83**, 034007 (2014).
[18]S. Y. Sun and J. L. Zhu, Phys. Rev. B **89**, 155403 (2014).
[19]S. C. Kim and S. R. E. Yang, Ann. Phys. **347**, 21 (2014).
[20]H. Y. Chen, V. Apalkov, and T. Chakraborty, Phys. Rev. Lett. **98**, 186803 (2007).
[21]G. Giavaras, P. A. Maksym, and M. Roy, J. Phys.: Condens. Matter **21**, 102201 (2009).
[22]G. Giavaras and F. Nori, Phys. Rev. B **85**, 165446 (2012).
[23]M. Amado, R. P. A. Lima, C. Gonzalez-Santander, and F. Dominguez-Adame, Phys. Rev. B **76**, 073312 (2007).
[24]R. P. A. Lima and M. Amado, J. Lumin. **128**, 858 (2008).
[25]E. Kasapoglu, H. Sari, U. Yesilgul, and I. Sokmen, J. Phys.: Condens. Matter **18**, 6263 (2006).
[26]H. Ham and H. N. Spector, J. Appl. Phys. **100**, 024304 (2006).
[27]M. Sahin, Phys. Rev. B **77**, 045317 (2008).
[28]M. Sahin, J. Appl. Phys. **106**, 063710 (2009).
[29]W. F. Xie, J. Lumin. **143**, 27 (2013).
[30]A. Delgado, A. Gonzalez, and D. J. Lockwood, Solid State Commun. **135**, 554 (2005).
[31]Q. H. Zhong, Eur. Phys. J. B **74**, 451 (2010).
[32]W. F. Xie, Phys. Lett. A **376**, 1657 (2012).